IMPLICATION FOR THE CORE-COLLAPSE SUPERNOVA RATE FROM 21 YEARS OF DATA OF THE LARGE VOLUME DETECTOR

N. Y. Agafonova[1], M. Aglietta[2], P. Antonioli[3], V. V. Ashikhmin[1], G. Badino[2,7], G. Bari[3], R. Bertoni[2], E. Bressan[4,5], G. Bruno[6], V. L. Dadykin[1], E. A. Dobrynina[1], R. I. Enikeev[1], W. Fulgione[2,6], P. Galeotti[2,7], M. Garbini[3], P. L. Ghia[8], P. Giusti[3], F. Gomez[2], E. Kemp[9], A. S. Malgin[1], A. Molinario[2,6], R. Persiani[3], I. A. Pless[10], A. Porta[2], V. G. Ryasny[1], O. G. Ryazhskaya[1], O. Saavedra[2,7], G. Sartorelli[3,4], I. R. Shakiryanova[1], M. Selvi[3], G. C. Trinchero[2], C. Vigorito[2,7], V. F. Yakushev[1], A. Zichichi[3,4,5,11]

(The LVD Collaboration)

[1] Institute for Nuclear Research, Russian Academy of Sciences, Moscow, Russia
[2] INFN-Torino, OATo-Torino, I-10100 Torino, Italy; vigorito@to.infn.it, fulgione@to.infn.it
[3] INFN-Bologna, 40126 Bologna, Italy
[4] University of Bologna, I-40126 Bologna, Italy
[5] Centro Enrico Fermi, I-00184 Roma, Italy
[6] INFN-Laboratori Nazionali del Gran Sasso and Gran Sasso Science Institute, I-67100 LAquila, Italy
[7] Dep. of Physics, University of Torino, I-10125 Torino, Italy
[8] CNRS-IN2P3, Paris, Laboratoire de Physique Nucléaire et de Hautes Energies (LPNHE),
Universités Paris 6 et Paris 7, France
[9] University of Campinas, 13083-859 Campinas, SP, Brazil
[10] Massachusetts Institute of Technology, Cambridge, MA 02139-4307, USA
[11] CERN, Geneva, Switzerland

ABSTRACT

The Large Volume Detector (LVD) has been continuously taking data since 1992 at the INFN Gran Sasso National Laboratory. The LVD is sensitive to neutrino bursts from gravitational stellar collapses with full detection probability over the Galaxy. We have searched for neutrino bursts in LVD data taken over 7,335 days of operation. No evidence of neutrino signals has been found between 1992 June and 2013 December. The 90% C.L. upper limit on the rate of core collapse and failed supernova explosions out to distances of 25 kpc is found to be 0.114 yr^{-1}.

Key words: methods: observational – neutrinos – supernovae: general

1. INTRODUCTION

The detection of neutrinos from the optically bright supernova in the Large Magellanic Cloud, SN 1987A, (Hirata et al. 1987; Bionta et al. 1987; Alekseev et al. 1987) and (Aglietta et al. 1987)[12] led to important inferences on the physics of core-collapse supernovae. It experimentally proved the critical role of neutrinos in the explosion of massive stars, as suggested more than 50 years ago (Gamow & Schoenberg 1940; Zel'dovich and Guseinov 1965; Colgate & White 1966; Nadyozhin 1977, 1978). Although a complete understanding of the physics involved is still lacking (see, e.g., Woosley & Janka 2005), the SN 1987A event helped to establish some aspects of the theory, namely, the total energy radiated, the neutrino temperatures, and the duration of the radiation pulse (see, e.g., Loredo & Lamb 2002; Pagliaroli et al. 2009b).

However, only a small number of neutrinos could be detected on that occasion, ≈ 20. Thus, it was not possible to study the detailed features of the neutrino emission, which is expected to carry important information on the dynamics of the explosion. Such a small number was due not only to the source distance (about 50 kpc from the Earth), but also to the relatively small dimensions of the detectors existing at that time. In fact, the need for larger and more sensitive neutrino detectors to study one of the most powerful and rare events occurring in the Galaxy had already become evident in the scientific community even before SN 1987A. The extremely low frequency (present estimates give a rate between one every 10 yr and one every 100 yr) implies that long-term observations using powerful neutrino detectors are essential to detect explosions of massive stars.

Also, the observation of neutrinos from SN 1987A was guided by the optical observation. However, the core-collapse rate in the Galaxy exceeds that of observable optical supernovae because light can be partially or totally absorbed by dust in the Galactic plane. In recent times, this point has been discussed by Adams et al. (2013) with the conclusion that large, long-term neutrino detectors are best suited to observe the Galaxy in the search for core-collapse supernovae explosions. Neutrino detectors are also sensitive to collapsing objects that fail to explode, becoming black holes (so-called failed supernovae), because those are expected to emit a neutrino signal even stronger, although shorter in time, than from core-collapse supernovae (Nakazato et al. 2008).

In addition, the prompt identification of a neutrino signal could provide astronomers with an early alert of a supernova occurrence (SuperNova Early Warning System, SNEWS (Antonioli et al. 2004), of which LVD is a founding member), allowing one to study phenomena like the shock breakout, a flash of radiation as the shock wave breaks out from the surface of the star (Klein & Chevalier 1978; Falk 1978), and to detect, for the first time directly, the signal due to the emission of gravitational waves (Pagliaroli et al. 2009a).

Based on the pioneering idea by Domogatsky & Zatsepin (1965), several neutrino detectors have been observing the Galaxy in the last decades to search for stellar collapses,

---

[12] The explanation of five signals recorded by the LSD detector about 5 hr earlier with respect to the other three experiments still remains controversial.

namely Super-Kamiokande (Ikeda et al. 2007), Baksan (Novoseltseva et al. 2011), MACRO (Ambrosio et al. 2004), AMANDA (Ahrens et al. 2002), and SNO (Aharmim et al. 2011). None of them has found evidence of supernovae explosions, thus setting limits on the rate of collapses. The longest duration experiment is Baksan: it has provided the most stringent limit in terms of rate (0.09 yr^{-1} at 90% C.L. based on 30 years of operation), but given the limited size its sensitivity to the whole Galaxy is controversial. In turn, the most sensitive detector, Super-Kamiokande (fully efficient up to 100 kpc), sets a limit on the rate of 0.32 yr^{-1} at 90% C.L.

In this paper, we present the results of the search for supernova neutrino bursts based on the data obtained by the Large Volume Detector (LVD; Aglietta et al. 1992a) in more than 20 yr of operation in the INFN Gran Sasso National Laboratory (LNGS) in Italy. The concept of a powerful neutrino detector was actually a basic motivation for the LNGS project, started at the end of the 1970s (see Bettini 1999; Zichichi 2000 for a historical review). The LVD is a large-mass (1,000 t), long-term (operating since 1992) neutrino experiment located at a depth of 3,600 m w.e. The detector's main characteristics are described in Section 2. The data set used in this work extends from 1992 June to 2013 December. In this period, the LVD has recorded more than 5 billion triggers, mostly due to radioactive background and atmospheric muons. In Section 3 we explain the criteria for reducing such backgrounds and selecting events that are potentially due to neutrinos. To search for supernova neutrino bursts, we analyze the time series of those events and search for clusters. While to provide the SNEWS with a prompt alert we use in the burst-search algorithm a fixed time window (20 s; Agafonova et al. 2008), in this work we consider different burst durations up to 100 s. The analysis is detailed in Section 4. In the same section we also discuss the sensitivity of the analysis to the recognition of a supernova event by using a conservative model based on the observations of neutrinos from SN 1987A (Pagliaroli et al. 2009b). Finally, in Section 5, we present the results of the search for neutrinos from gravitational stellar collapses happening in the whole Galaxy. Our conclusions are given in Section 6.

2. THE LARGE VOLUME DETECTOR

The LVD[13] is a 1,000 t liquid scintillator experiment aimed at detecting O(MeV) and O(GeV) neutrinos, both of astrophysical origin (like those from supernova explosions) and from accelerators (like those from the CNGS beam; see, e.g., Agafonova et al. 2012). Neutrinos can be detected in LVD through charged current (CC) and neutral current (NC) interactions on protons, carbon nuclei, and electrons of the liquid scintillator. The scintillator detector is supported by an iron structure, whose total mass is about 850 t. This can also act as a target for neutrinos and antineutrinos because the product of interactions in iron can reach the scintillator and be detected (Agafonova et al. 2007). The total target thus consists of 8.3 × 10^{31} free protons, 4.3 × 10^{31} C nuclei, and 3.39 × 10^{32} electrons in the scintillator and of 9.7 × 10^{30} Fe nuclei in the support structure. The main neutrino reaction in LVD is the inverse beta decay (IBD), as can be seen in Table 1, where all other relevant neutrino interaction channels are shown too.

---

[13] LVD is the successor to the Mont Blanc LSD detector (Aglietta et al. 1992b).

Table 1
The ν Interaction Channels in LVD

	ν Interaction Channel	E_ν Threshold	%
1	$\bar{\nu}_e + p \rightarrow e^+ + n$	(1.8 MeV)	(88%)
2	$\nu_e + {}^{12}C \rightarrow {}^{12}N + e^-$	(17.3 MeV)	(1.5%)
3	$\bar{\nu}_e + {}^{12}C \rightarrow {}^{12}B + e^+$	(14.4 MeV)	(1.0%)
4	$\nu_i + {}^{12}C \rightarrow \nu_i + {}^{12}C^* + \gamma$	(15.1 MeV)	(2.0%)
5	$\nu_i + e^- \rightarrow \nu_i + e^-$	(-)	(3.0%)
6	$\nu_e + {}^{56}Fe \rightarrow {}^{56}Co^* + e^-$	(10. MeV)	(3.0%)
7	$\bar{\nu}_e + {}^{56}Fe \rightarrow {}^{56}Mn + e^+$	(12.5 MeV)	(0.5%)
8	$\nu_i + {}^{56}Fe \rightarrow \nu_i + {}^{56}Fe^* + \gamma$	(15. MeV)	(2.0%)

Note. Cross sections of different interactions are obtained referring to Strumia & Vissani (2003) for interaction 1, Fukugita et al. (1988) for interactions 2–4, Bahcall et al. (1995) for interaction 5, and Kolbe & Langanke (2001) and Toivanen et al. (2001) for interactions 6–8.

The LVD consists of an array of 840 scintillator counters, 1.5 m^3 each, viewed from the top by three photomultipliers (PMTs). It is a modular detector. From the viewpoint of the PMT power supply, trigger, and data acquisition, the array is divided in sectors (dubbed *towers*): each sector operates independently of the others. Each tower includes 280 counters, divided in four *groups* of 80, 80, 64, and 56 counters: they share the same low-voltage power supplies. Moreover, for each tower, counters are organized in 35 *modules* of eight that are at the same position in the array. Those share the same charge digitizer board (Bigongiari et al. 1990) and the same high-voltage divider. This modularity allows LVD to achieve a very high duty cycle, which is essential in the search for unpredictable sporadic events. On the one hand, the three independent data acquisition systems, one per tower, minimize (in practice, nullify) the probability of a complete shutdown of the experiment. On the other hand, failures involving one or more counters do not affect other counters. The LVD can thus be serviced during data taking by stopping only the part of the detector (down to individual counters) that needs maintenance. The modularity of the detector results in a "dynamic" active mass M_{act}, as we will see in Section 3.1.

The LVD has been in operation since 1992 June 9, its mass increasing from 300 t (about one full "tower") to its final one, 1,000 t, in 2001 January. In the following analysis, we consider data recorded between 1992 June 9 and 2013 December 31. During this period, the LVD has been running in two different conditions due to different values of the trigger threshold. The trigger logic (extensively described in Agafonova et al. 2008) is based on the threefold coincidence of the PMTs in a single counter. Given the relevance of the IBD reaction, the trigger has been optimized for the detection of both products of this interaction, namely the positron and the neutron. Each PMT is thus discriminated at two different threshold levels, the higher one, $\mathcal{E}_H$, being also the main trigger condition for the detector array. The lower one ($\mathcal{E}_L \simeq 0.5$ MeV) is in turn active only in a 1 ms time window following the trigger, allowing the detection of n, p captures. Between 1992 June 9 and 2005 December 31 (period P1), $\mathcal{E}_H$ was set to 5 MeV for core counters, i.e., counters not directly exposed to the rock radioactivity (about 47% of the total), and to 7 MeV for external ones. From 2006 January 1 onward (period P2), $\mathcal{E}_H$ was set to 4 MeV for all

Table 2
Data Set Features in Periods P1 and P2

	$R_{\rm tot}$ $(\text{s}^{-1} \times \text{t}^{-1} \times 10^{-4})$	$R_7 (E \geqslant 7\,\text{MeV})$ $(\text{s}^{-1} \times \text{t}^{-1} \times 10^{-4})$	$R_{10} (E \geqslant 10\,\text{MeV})$ $(\text{s}^{-1} \times \text{t}^{-1} \times 10^{-4})$	$R_{\rm L} (E \geqslant 0.5\,\text{MeV})$ $(\text{s}^{-1} \times \text{t}^{-1} \times 10^{-4})$	$M_{\rm act}$ (t)	Exposure (t $\times$ y)	$t_{\rm live}$ (days)	$t_{\rm live} (M_{\rm act} \geqslant 300\,\text{t})$ (days)
P1	50	1.4	0.28	2.4×10^6	576	7320	4636	4419
P2	130	2.0	0.26	2.5×10^6	946	7560	2916	2916

Note. $R_{\rm tot}$ is the total trigger rate, R_7, R_{10}, and $R_{\rm L}$ are the rates of events with energy above 7, 10, 0.5 MeV, respectively, and $M_{\rm act}$ Is the average active mass.

counters, independent of their location. The lower threshold has instead remained constant in both periods.

Once a trigger is identified, the charge and time of the three summed PMT signals are stored in a memory buffer. The time is measured with a relative accuracy of 12.5 ns and an absolute one of 100 ns (Bigongiari et al. 1990). At 1 ms after the trigger, all memory buffers are read out independently in the three towers. The mean trigger rate is $\approx$0.005 s^{-1}t^{-1} in period P1 and $\approx$0.013 s^{-1}t^{-1} in period P2, as shown in Table 2 with other features of the two periods of data taking.

3. EVENT SELECTION

The method used in LVD to search for neutrino bursts from gravitational stellar collapses essentially consists of searching, in the time series of single counter signals (events), for a sequence (cluster) whose probability of being simulated by fluctuations of the counting rate is very low (see Section 4). The higher the event frequency, the higher is the probability of a "background cluster," given by accidental coincidences. At the trigger level, the bulk of events in the LVD are due to natural radioactivity products, both from the rock surrounding the detector and from the material that constitutes the detector itself, and to atmospheric muons. The set of cuts described in this section aims at reducing such a background while isolating signals potentially due to neutrinos. The first condition (Section 3.1) functions as a filter to remove events triggered in malfunctioning counters. The second and third conditions (Section 3.2) reject cosmic-ray muons and most of the radioactive background. The fourth one (Section 3.3) refines the rejection of defective counters through the analysis of the time series of the events. As we will show below, after the background reduction, the counting rate is decreased by a factor of about 400.

3.1. Counter Selection (Basic Cuts)

The first step in the selection chain is the identification of well-operating counters, i.e., the rejection of signals detected in defective ones. Indeed, the participation of a counter to a trigger does not guarantee that it functions well. To this aim, we exploit the response of counters to cosmic-ray muons. Muons are identified through the time coincidence of signals in two or more counters. The average rate of muons crossing LVD, $f_\mu(\text{LVD})$, is $0.097 \pm 0.010\,\text{s}^{-1}$, the measured rate for each counter, $f_\mu(c)$, being $5 \times 10^{-4}\,\text{s}^{-1}$ (i.e., 1.8 hr^{-1}). The distribution of energy losses of muons in each counter is also monitored: due to the low rate, a muon spectrum is built every month. Quality cuts to be applied to counters (and hence to events) are then defined on the basis of muon rate and energy spectra. Namely, we use a counter in the rest of the analysis if $f_\mu(c) \geqslant 3 \times 10^{-5}\,\text{s}^{-1}$ and if the monthly energy spectrum is

consistent with a reference one. Moreover, we require that the counting rate above 7 MeV (corresponding to the high-energy threshold in period P1) is less than $3 \times 10^{-3}\,\text{s}^{-1}$ during the last two hours of operation (Agafonova et al. 2008). We have verified indeed that high rates usually correspond to faulty electronic or badly calibrated counters, i.e., counters in need of maintenance. Note that such a cut usually involves a very small amount of counters, 2% on average.

The active detector mass, $M_{\rm act}$, resulting after applying the described cuts is shown in Figure 1 as a function of time in the data period considered in the present analysis.

3.2. Neutrino Event Selection

The next level in the event selection concerns the suppression of the muonic and radioactive background. To this aim, the following cuts are applied.

1. Events characterized by signals in two or more counters within 175 ns are rejected as muons. Furthermore, to avoid contamination by any signal associated with muon interactions inside the detector or in the surrounding rock, a dead time of 1 ms is applied after each muon event. The total dead time introduced by this cut is $t_{\rm dead} \leqslant 0.01\%$, corresponding to less than 1 hr yr^{-1}. The probability of rejecting a neutrino candidate involving more than one counter has been evaluated in Antonioli et al. (1991). Convolving this probability with the neutrino energy spectra expected from a core-collapse supernova, we obtain that about 3% of neutrino interactions are erroneously rejected. Note that, in the case of a positive neutrino burst identification, these events can be recovered.

2. Only events whose associated energy is in the range $10\,\text{MeV} \leqslant E_{\rm signal} \leqslant 100\,\text{MeV}$ are considered. This interval is chosen not only with respect to the expected neutrino energy distribution in the case of supernova explosions (see, for example, Pagliaroli et al. 2009b) but also because it allows us the suppression of most of the radioactive background. In turn, the effect on the expected neutrino signal is small ($\sim$15%) because of the energy dependence of neutrino cross sections.

After applying the described cuts, the event rate is strongly reduced to about $3 \times 10^{-5}\,\text{s}^{-1}$t^{-1}. As shown in Figure 2, it is stable over time and almost independent of the hardware configuration. Indeed, the effect due to the threshold change between the two periods P1 and P2 is negligible, as shown in Table 2, where relevant features of the two periods are listed. The average frequencies $R_{10} = f(E \geqslant 10\,\text{MeV})$ and $R_{\rm L} = f(E \geqslant 0.5\,\text{MeV})$ are consistent in both periods. The integral energy spectra of the signals, after quality cuts in the energy range 10–100 MeV, are also shown in Figure 3 for the two periods. The slightly higher frequency in period P1 is due to the the lower muon discrimination power as a consequence of the smaller active mass. We can conclude that a joint analysis of data taken in the two periods is appropriate.
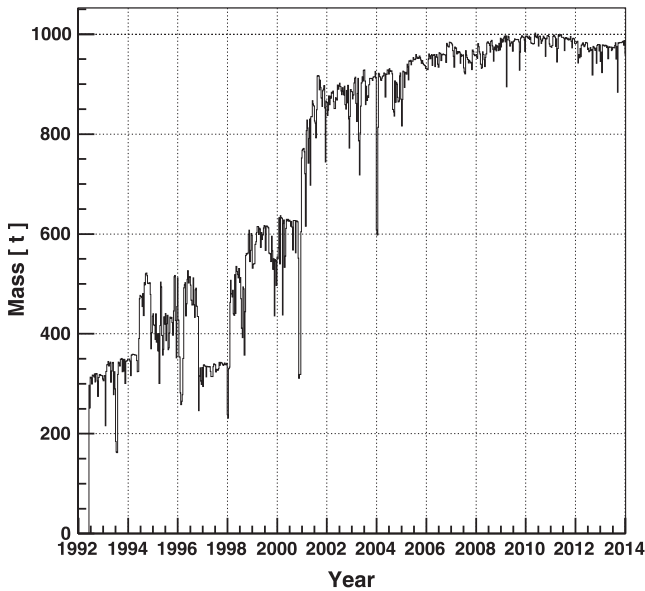
Figure 1. LVD active mass as a function of time in the period from 1992 June to 2013 December.
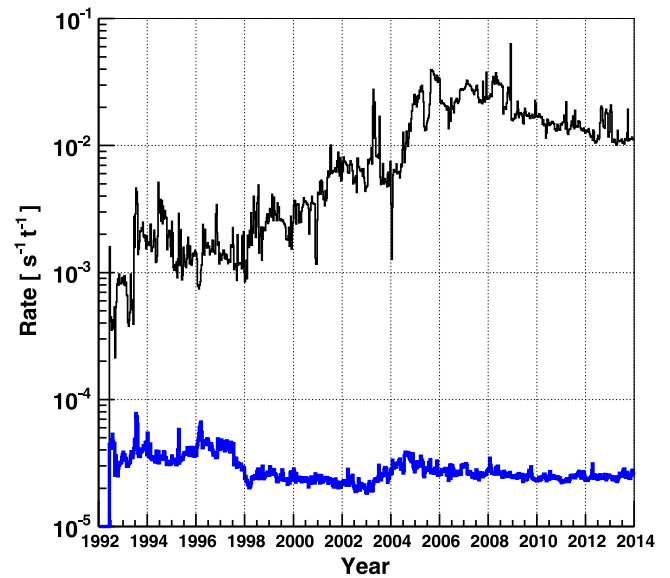

Figure 2. LVD counting rate as a function of time in the period from 1992 June to 2013 December. The thin black curve shows the trigger rate, and the thick blue one shows the rate after the suppression of the muon and radioactive background (see Section 3.2).

3.3. Counter Selection (Topological Cuts)

The final set of selection cuts is introduced during the time analysis of the events surviving the previous filters. As we will see in Section 4.2, the search for neutrino bursts in the LVD consists of searching for clusters of events within a certain time window with duration Δt up to 100 s in steps of 100 ms. Every cluster is characterized by Δt and by the number of events, m (multiplicity), within Δt. In the case of a neutrino burst, we expect the m events to be distributed uniformly over the array, thanks to the energy cut at 10 MeV that guarantees the uniformity of the response of the counters against threshold effects. If among the m events there is an excess of signals in specific counters, or in eight-counter modules, or in counter groups, then events from that counter (module, group) are rejected. The following cuts, dubbed "topological" because they check the spatial distribution of events, are meant to discard detector components that are temporarily unstable, due for example to electric noise or to maintenance activities in the experiment.

We first check the occurrence of single counters in each cluster of events. If m is the cluster multiplicity and N_c the number of active counters, a counter is excluded from the cluster if its occurrence n_c corresponds to a Poisson probability $P(k \geqslant n_c, m/N_c) \leqslant 1 \times 10^{-5}$. Then we check the occurrence of each eight-counter module in every cluster. The cut on modules is analogous to the one on counters: the probability of determining the exclusion is in this case scaled by a factor of eight, i.e., $P = 8 \times 10^{-5}$. Finally, we apply the same logic as above to check the occurrence of each counter group in every cluster of events. The probability of rejecting a group is now scaled by a factor of 70, i.e., $P = 70 \times 10^{-5}$. We note that the sequence of cuts is applied to each cluster of events separately. Also, each cluster is reanalyzed every time a cut (on counters, modules, or groups) is applied; that is, the cluster multiplicity m is reevaluated at each step of the sequence.

The significance of a cluster (given by its frequency of imitation due to background fluctuations) depends on Δt and m (see Section 4.2). Because "topological" cuts might affect
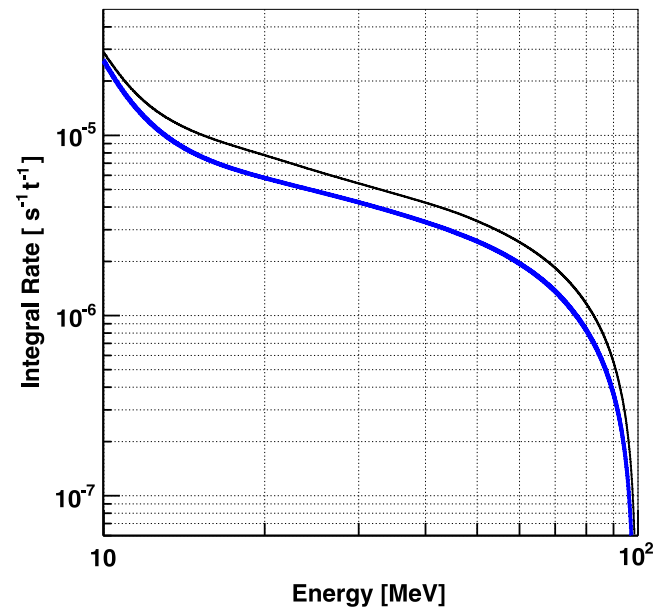
Figure 3. Integral energy spectra of signals detected in periods P1 (black thin line) and P2 (blue thick line).

(reduce) m[14], we have carefully monitored their incidence on data over time. In particular, we have inspected every cluster that had a rather low imitation frequency (less than one per month), i.e., rather high significance, before applying topological cuts. Most of them correspond to periods of electronics problems, in particular of time-to-digital converters (TDCs). Malfunctions of TDCs can spuriously increase the multiplicity

---

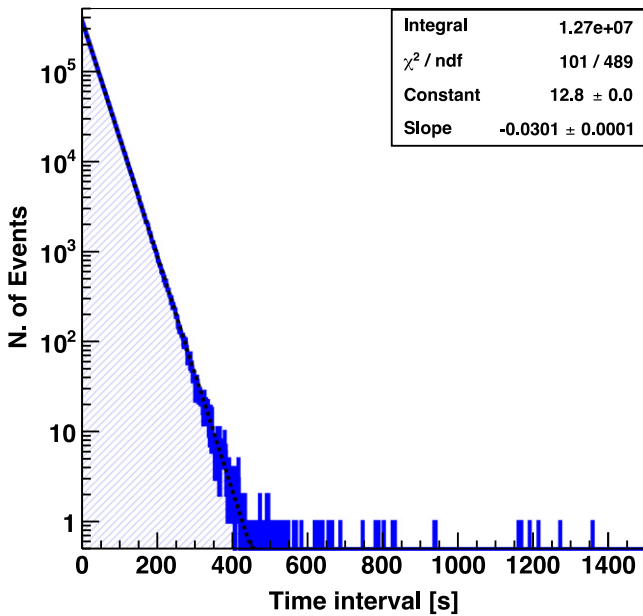[14] In Section 4.3 we will quantify the effect of these cuts on a possible real neutrino signal.

Figure 4. Distribution of normalized time intervals between successive events passing the selections described in the text. The normalization is done by equalizing the counting rate at the time of each event to the average one. The dashed black line shows the result of a Poissonian fit to the distribution.

of a cluster: muons are not rejected properly (see Section 3.2) and are identified as neutrino candidates.

4. SEARCH FOR NEUTRINO BURSTS

In this section we describe the analysis performed on the events satisfying the selection criteria described above. The aim is to search for significant clusters of events that could be indicative of neutrino bursts. The prerequisite to determine the significance is that the counting rate behavior is Poissonian: this is shown in Section 4.1, by studying the time distribution of the selected events. The search for clusters of events, together with the determination of their statistical significance, is detailed in Section 4.2. The sensitivity of LVD to the detection of neutrino bursts resulting from the described analysis is finally discussed in Section 4.3.

4.1. Time Distribution of the Data Set

The search for neutrino bursts is performed on data spanning the period from 1992 June 9 to 2013 December 31. During this time, the active mass has been larger than 300 t over 7,335 days, corresponding to a live time larger than 93% (>99% since 2001). Here, 300 t is the minimal mass that allows LVD to be sensitive to neutrino bursts over the whole Galaxy (see Section 4.3). The number of events collected in this period and passing the cuts described in the previous section is 12,694,637. The distribution of time intervals between successive events is shown in Figure 4 (blue histogram). Because of the variable detector configuration, the differences in time have been normalized to account for the active mass at the time of the events. The normalization is done by equalizing the event rate (f, which depends on the active mass) to a reference one, f_{ref}, that corresponds to the average one when the whole array (1,000 t) is in operation, i.e., $\delta t_{norm} = \delta t \cdot f / f_{ref}$, with $f_{ref} = 0.03 \, \mathrm{s}^{-1}$. The LVD events behave as a stochastic

time series well described by the Poisson statistics, as proved by the quality of the fit to a Poisson distribution (shown in the figure as a dashed black line).

4.2. Analysis Method

The search for neutrino bursts in LVD data is essentially a two-step process.

In the first step, we analyze the entire time series[15] to search for a cluster of events. The rationale of the search is that each event could be the first of a possible neutrino burst. Because we do not know a priori the duration of the burst, we consider all clusters formed by each event and the n successive ones, with n ranging from 1 to all those contained inside a time window $\Delta t_{max} = 100$ s. The duration of each cluster is given by the time difference Δt between the first event and the last one of each sequence. The analysis is then applied iteratively, starting from the next one, to all LVD events. The advantage of the described analysis, where all clusters with durations up to 100 s are considered, is that it is unbiased with respect to the duration of the possible neutrino burst, unknown a priori. Moreover, the choice of $\Delta t_{max} = 100$ s is very conservative because it well exceeds the expected duration of a neutrino burst from core-collapse supernovae and even more that from failed supernovae.

The second step of the process consists of deciding if one or more among the detected clusters are neutrino-burst candidates. To this aim, we associate with each of them (characterized by m_i, Δt_i) a quantity that we call the imitation frequency, F_{im_i}. This represents the frequency with which background fluctuations can produce clusters of any duration, between zero and Δt_{max}, with the same or lower probability than that of the individual cluster. As shown in (Fulgione et al. 1996), this quantity, which depends on (m_i, Δt_i), on the background rate, f_{bk_i}, and on the maximum cluster duration chosen for the analysis, Δt_{max}, can be written as

$$F_{im_i} = f_{bk}^2 \, \Delta t_{max} \sum_{k \geqslant m_i - 2} P\left(k, f_{bk_i} \Delta t_i\right). \tag{1}$$

Given the duration of the LVD data set (more than 20 yr), we choose $1/100 \, \mathrm{yr}^{-1}$ as the imitation-frequency threshold, F_{im}^{th}. That means that a cluster (m_i, Δt_i) is considered as a candidate neutrino burst if

$$\sum_{k \geqslant m_i - 2} P\left(k, f_{bk} \Delta t_i\right) < \frac{F_{im}^{th}}{f_{bk}^2 \cdot \Delta t_{max}}, \tag{2}$$

where $P(k, f_{bk} \Delta t_i)$ is the Poisson probability to have k events in the time window Δt_i if f_{bk} is the average background frequency.

The introduction of the imitation frequency has a double advantage. From the viewpoint of the search for neutrino bursts, it allows us to define a priori the statistical "significance" of each cluster in terms of frequency. Also, it allows us to monitor the performance of the search algorithm and the

---

[15] We choose here not to exploit the capability of LVD to detect both products of the IBD reaction (see Section 3). Indeed, as discussed in (Agafonova et al. 2008), the algorithm applied to all selected events is more sensitive than when applied to events with the IBD signature. It becomes slightly more efficient if we apply it to a mixture of unsigned and signed events, but at the price of loss of simplicity and of independence from models. Finally, by using all events, the algorithm is sensitive not only to possible neutrino interactions in the liquid scintillator but also in the iron structure (Imshennik & Ryazhskaya 2004).
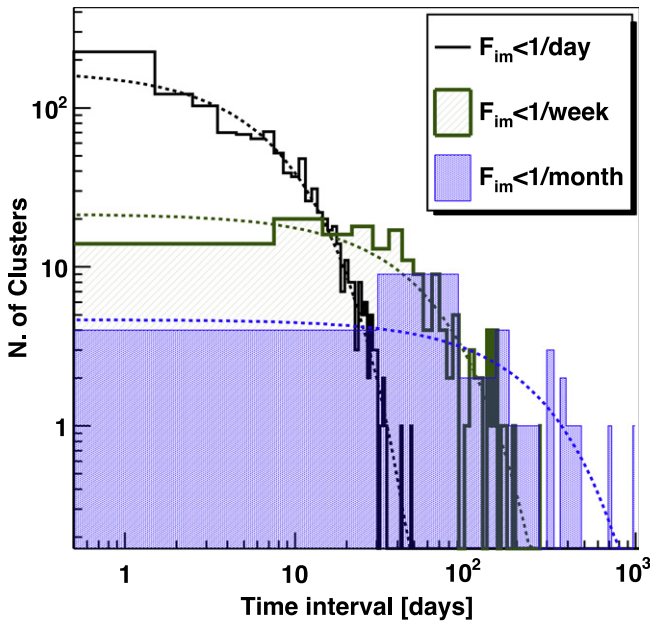
Figure 5. Distributions of time intervals between consecutive clusters (solid lines) fitted by Poisson laws (dashed lines) for imitation frequencies $F_{im} < 1/$ day (black), 1/week (green), and 1/month (blue).
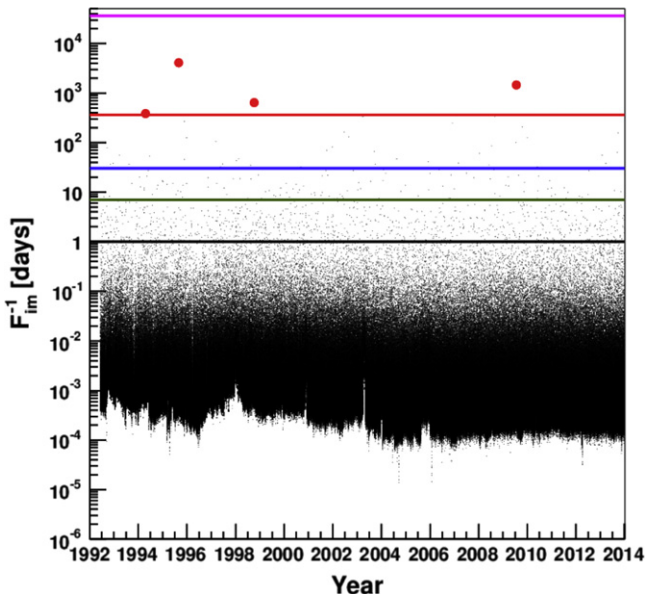

Figure 6. Distribution of detected clusters versus time between 1992 June and December 2013. Red dots represent clusters with imitation frequency less than $F_{im} = 1/$year. Black, green, blue, red, and purple lines correspond to $F_{im}^{th} = 1/$ day, $F_{im}^{th} = 1/$ week, $F_{im}^{th} = 1/$ month, $F_{im}^{th} = 1/$ y, and $F_{im}^{th} = 1/100$ y, respectively.

stability of the detector[16] by increasing the imitation-frequency threshold. Namely, we study the time distribution of clusters (i.e., the difference in time between clusters) having an imitation frequency less than one per day, one per week, and

one per month. The numbers of clusters detected over 7,335 days are 1123, 165, and 45, respectively. Note that these rates are definitely lower than the corresponding frequency limits (7335, 1048, and 245, respectively). In Figure 5 we show the distributions of time differences between consecutive clusters for the three different values of imitation frequency ($F_{im} < 1$ day^{-1}, week^{-1}, month^{-1} as black, green, and blue histograms, respectively). The superimposed dotted lines are the result of a Poissonian fit to each distribution. The good agreement between the data and the expected Poissonian behavior shows that the search algorithm and the detector are under control over the whole period of data taking. Also, the occurrence of clusters with different F_{im} over the 7,335 days of measurement is uniform, as can be seen in Figure 6. It shows the F_{im} of all detected clusters as a function of time. Clusters above the black, green, and blue lines are those with $F_{im} < 1$ day^{-1}, week^{-1}, and month^{-1}, respectively.

4.3. Analysis Sensitivity

The capability of LVD to detect in real time (i.e., "online") a supernova event is extensively discussed in Agafonova et al. (2008). In that case, a time window (i.e., 20 s) is used in the burst-search algorithm. In turn, for the present analysis (so-called "offline"), we do not fix a priori the duration of the burst: we consider all possible durations up to 100 s. Consequently, we extend here our previous study to account for this choice. As in Agafonova et al. (2008), we discuss the sensitivity to the identification of a neutrino burst in terms of the maximum detectable distance of the supernova explosion.

To estimate the characteristics of a neutrino signal in LVD from a gravitational stellar collapse, we exploit the parameterization of the neutrino flux proposed by Pagliaroli et al. (2009b). That is based on the analysis of neutrinos observed at the occurrence of SN 1987A, and it includes the effect of neutrino oscillations too. The adopted model can be summarized as follows:

1. The neutrino emission occurs in two main stages:[17] ν_e and $\bar{\nu}_e$ are emitted during the accretion phase ($\approx$500 ms), determining in part the future evolution of the core collapse (O'Connor & Ott 2011); neutrinos and antineutrinos, ν_i and $\bar{\nu}_i$, of all flavors are emitted during the thermal cooling.

2. The total neutrino signal is expected to develop on a timescale of about 10 s, being 90% (50%) of the detected events in the first 10 s (1 s).

3. The time-averaged temperatures of emitted neutrinos are 10.7 MeV for ν_e, 12.0 MeV for $\bar{\nu}_e$, and 14.2 MeV for $\nu_{\mu,\tau}$, $\bar{\nu}_{\mu,\tau}$.

4. Mikheev-Smirnov-Wolfenstein (MSW) oscillation effects on neutrinos crossing the matter of the collapsing star (Wolfenstein 1978), (Mikheev & Smirnov 1985) are taken into account, and ν–ν interactions are neglected (Agafonova et al. 2007). The normal mass hierarchy scenario has been conservatively assumed together with the most recent values of θ_{12} and mass-squared differences Δm_{12}^2 and Δm_{23}^2 (see, e.g., Strumia & Vissani 2010 for a review). In this scenario, the nonnull value for the θ_{13} mixing angle (An et al. 2012) has no significant effect on the expected neutrino signal.

By simulating neutrino events in the LVD generated according to the described model, we estimate the detection

---

[16] The performance of the selection procedure and its capability to discriminate a burst from background fluctuations has also been hardware tested, by generating clusters of signals in a subset of counters equipped with an LED system.

[17] The ν_e emitted in shock breakout, when the ν_e produced in electron captures (neutronization) are released, play a secondary role in the detector sensitivity.
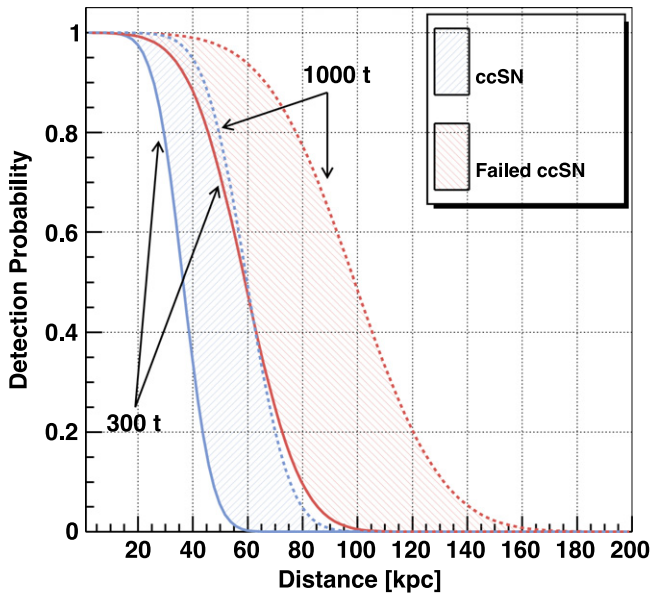
Figure 7. LVD detection probability versus source distance for the imitation frequency of $1/100 \ \mathrm{yr}^{-1}$ (see text). The blue and red bands correspond to the case of standard core-collapse (ccSN) and failed supernovae, respectively. The solid (dashed) line represents an active mass of 300 (1000) t.

probability as a function of the distance of the gravitational stellar collapse from the Earth. We find that a total of more than 300 events would trigger LVD for a collapse 10 kpc away: events are shared among all interaction channels, as shown in Table 1. This number becomes more than 260 when taking into account the chosen energy cut at $10 \ \mathrm{MeV}$[18]. The detection probability as a function of the distance of the collapse is shown in Figure 7 for the chosen imitation frequency of $1/100 \ \mathrm{yr}^{-1}$. The blue band corresponds to the case of a standard core-collapse supernovae: the solid (dashed) line represents an active mass of 300 (1,000) t.

We also evaluate the detection probability in the case of stellar collapses ending in black holes, so-called failed supernovae, by using a similar procedure as above. This is shown as a red band in the same Figure 7 (similarly, the two boundary lines represent masses of 300 t and 1,000 t). In this case, we take as reference the predictions of Nakazato et al. (2008) by choosing the most conservative one in terms of neutrino emission. Namely, we assume a progenitor of 40 solar masses, a burst duration shorter than 500 ms, a total emitted energy in neutrinos of 1.3×10^{53} ergs, and the inverted neutrino mass hierarchy.

We can conclude that the LVD efficiency in detecting supernovae or failed supernovae explosions is more than 95% for distances less then 25 kpc when the detector active mass is larger than 300 t.

5. RESULTS

By analyzing the time series of 12,694,637 events (selected as described in Section 3 and collected over 7,335 days of data

taking), we get 26,914,419 clusters with multiplicity $m \geqslant 2$ and $\Delta t \leqslant 100$ s (12,199,631 during P1 and 14,714,788 during P2). They are shown in Figure 8 in a two-dimensional graph whose axes are the cluster duration, Δt, and the multiplicity[19], m^*.

For each cluster, we evaluate the imitation frequency, $F_{\mathrm{im}}^{\mathrm{th}}$, following Equation 1. Those are shown in Figure 6 as a function of time. In both Figures 6 and 8 the purple line represents the expectations for an $F_{\mathrm{im}}^{\mathrm{th}}$ of $1/100 \ \mathrm{yr}^{-1}$, i.e., the threshold for considering a cluster as a neutrino-burst candidate (see Section 4.2). None of the observed clusters passes such a threshold, the maximum detected significance being $(F_{\mathrm{im}})^{-1} = 11.16$ yr associated with a cluster of seven events during about 5 s. For the sake of completeness, we have carefully inspected all clusters with $F_{\mathrm{im}} \leqslant 1/\mathrm{month}$ (45 of them). Their energy spectra have been examined, as well as the number of low-energy delayed signals that might be the signature of IBD interactions (see Section 2). All 45 clusters are fully compatible with chance coincidences among background signals. The characteristics of the four most significant among them ($F_{\mathrm{im}} \leqslant 1/\mathrm{year}$) are reported in Table 3. Besides the date, we show the conditions of the detector at the time of the cluster, i.e., the active mass and background frequency. The properties of the clusters are listed in the last five columns: multiplicity, duration, imitation frequency, average energy of events, and number of IBD candidate events. The distance corresponding to a 90% detection probability is also shown: it is derived from the blue curve in Figure 7 taking into account the active mass. We note that for all four clusters it is well above 25 kpc.

We conclude that no evidence is found for core-collapse or failed supernovae during the considered data-taking period. Taking into account the live time of 7335 days, we obtain a limit on the rate of gravitational collapses out to 25 kpc of less than 0.114 per year at 90% C.L.

6. CONCLUSIONS

In this paper we have presented the results of the search for neutrino-burst signals from supernovae explosions performed with LVD data taken over more than 20 yr, from 1992 June 9 to 2013 December 31.

The neutrino-burst detection technique is based on the search for a sequence of candidate neutrino events whose probability of being simulated by fluctuations of the counting rate is very low. As the latter is dominated by the background of atmospheric muons and natural radioactivity products, we have developed a set of selection criteria to isolate signals that are more probably due to neutrinos. Such a selection is based on the topology and energy of the events. Also, given the large number of detectors and the long time of operation, we have been very careful in identifying ill-functioning or unstable ones

---

[18] As anticipated in Section 3.3, the described simulation allows us to also evaluate the possible effect of topological cuts on a real neutrino burst. It results that, even in the worst possible experimental conditions, i.e., for a source at 25 kpc and a minimal detector active mass, $M_{\mathrm{act}} = 300$ t, the probability of mistakenly rejecting counters, modules, or groups due to statistical fluctuations of a uniform distribution, thus downgrading an authentic cluster, remains always $< 3 \times 10^{-4}$.

[19] Here, m^* is the multiplicity corrected to account for the background frequency, f_{bk_i}, at the time of each cluster. The correction is done by equalizing f_{bk_i} to the average rate $f_{\mathrm{bk}_0} = 0.03 \ \mathrm{s}^{-1}$ (see Sections 3.2 and 4.1). Then, m^* is obtained by the numerical solution of the equation

$$\frac{P\left[k \geqslant \left(m_i^* - 2\right), f_{\mathrm{bk}_0} \cdot \Delta t_i\right]}{P\left[k \geqslant \left(m_i - 2\right), f_{\mathrm{bk}_i} \cdot \Delta t_i\right]} = \frac{f_{\mathrm{bk}_0}^2}{f_{\mathrm{bk}_i}^2},$$

where $P(k \geqslant (m_i - 2), f_{\mathrm{bk}_i} \cdot \Delta t_i)$ is the Poisson probability to have clusters of multiplicity $k \geqslant (m_i - 2)$, and $(f_{\mathrm{bk}_i} \cdot \Delta t_i)$ is the average multiplicity.

Table 3
Characteristics of Clusters with Significance $F_{im} < 1 \times yr^{-1}$

n.	UTC	M_{act} (t)	f_{bk} (s^{-1})	$D_{90\%}$(kpc)	m	Δt (s)	$F_{im}^{-1}(y)$	$\bar{E}$ (MeV)	N_{IBD}
1	1994 16 Apr 10:40:49.263	346	1.08×10^{-2}	29.5	7	18.88	1.06	26.5	2
2	1995 27 Aug 16:18:10.478	431	1.85×10^{-2}	35.0	7	5.49	11.16	36.2	1
3	1998 7 Oct 15:41:41.775	552	1.40×10^{-2}	30.6	12	90.05	1.76	32.2	3
4	2009 18 Jul 7:39:20.517	976	2.40×10^{-2}	40.4	12	42.71	4.02	14.6	1

Note. Time of occurrence (UTC), active mass (M_{act}), background rate (f_{bk}), distance corresponding to 90% detection probability ($D_{90\%}$), multiplicity (m), duration (Δt), inverse of imitation frequency (F_{im}^{-1}), average events energy ($\bar{E}$), number of IBD candidates (N_{IBD}).

over time. After the selection, the background rate is reduced by a factor of about 400, leaving us with almost 13 million events.

To search for candidate neutrino bursts among them, we have searched for all possible clusters of events with durations up to 100 s. That makes our search model-independent because the duration of a neutrino burst due to a supernova explosion is unknown. The knowledge of the background as well as its long-term stability are of essence in evaluating the probability of each found cluster. We have shown that the counting rate is stable over the period of observation and that its behavior is Poissonian. That has allowed us to associate with each candidate burst an a priori significance, which we have chosen to give in terms of imitation frequency, F_{im}. Given the total time of observation, we have fixed a threshold to F_{im}^{th} of 1/100 yr^{-1} for considering a cluster as a real neutrino burst. We have shown that, with the adopted method of analysis and with the chosen threshold, the LVD is fully efficient to gravitational collapses (due to supernovae explosions or failed supernovae) within a radius of 25 kpc from earth, even when its mass is only one-third (300 t) of its full one (1000 t).

Out of the 27 million detected clusters, we have found that none has an imitation frequency less than 1/100 yr^{-1}. We have thus concluded that no evidence has been found for core-collapse supernovae occurring up to 25 kpc during the period of observation[20]. Finally, we have set a limit of less than 0.114 collapses per year at 90% C.L., this being the most stringent limit ever achieved by the observation of supernovae through neutrinos in the entire Galaxy.

Figure 8. Distribution of detected clusters in the space (Δt, m^*). Red dots represent clusters with imitation frequency less than $F_{im} = 1$ yr^{-1}. The purple line corresponds to $F_{im}^{th} = 1/100$ yr^{-1}.

Gianni Navarra, and Georgiy T. Zatsepin: we are left with their memory and their teachings.

REFERENCES

Adams, S. M., Kochanek, C. S., Beacom, J. F., Vagins, M. R., & Stanek, K. Z. 2013, ApJ, 778, 164
Agafonova, N. Y., Aglietta, M., Antonioli, P., et al. 2007, APh, 27, 254
Agafonova, N. Y., Aglietta, M., Antonioli, P., et al. 2008, APh, 28, 516
Agafonova, N. Y., Aglietta, M., Antonioli, P., et al. 2012, PhRvL, 109, 070801
Aglietta, M., Alpat, B., Alyea, E. D., et al. 1992a, NCimA, 105, 1793
Aglietta, M., Antonioli, P., Badino, G., et al. LSD Collaboration 1992b, APh, 1, 1
Aglietta, M., Badino, G., Bologna, G., et al. 1987, EL, 3, 1315
Aharmim, B., Ahmed, S. N., Anthony, A. E., et al. SNO Collaboration 2011, ApJ, 728, 83
Ahrens, J., Bai, X., Barouch, G., et al. 2002, APh, 16, 345
Alekseev, E. N., Alekseeva, L. N., Volchenko, V. I., & Krivosheina, I. V. 1987, JETPL, 45, 589
Ambrosio, M., Antolini, R., Baldini, A., et al. 2004, EPJC, 37, 265
An, F. P., Bai, J. Z., Balantekin, A. B., et al. 2012, PhRvL, 108, 171803
Antonioli, P., Fienberg, R. T., Fleurot, F., et al. 2004, NJPh, 6, 114
Antonioli, P., Fulgione, W., Galeotti, P., & Panaro, L. 1991, NIMPA, 309, 569
Bahcall, J. N., Kamionkowski, M., & Sirlin, A. 1995, PhRvD, 51, 6146
Bettini, A. 1999, in The Gran Sasso Laboratory 1979–1999: a vision becomes reality (Assergi: Laboratori Nazionali del Gran Sasso)
Bigongiari, A., Fulgione, W., Passuello, D., Saavedra, O., & Trinchero, G. 1990, NIMPA, 288, 529

---

[20] During this time, the results of the search have been communicated every two years at International Cosmic Ray Conferences (LVD Collaboration 1993, 1995, 1997, 1999, 2001, 2003, 2005, 2007, 2009, 2011, 2013).
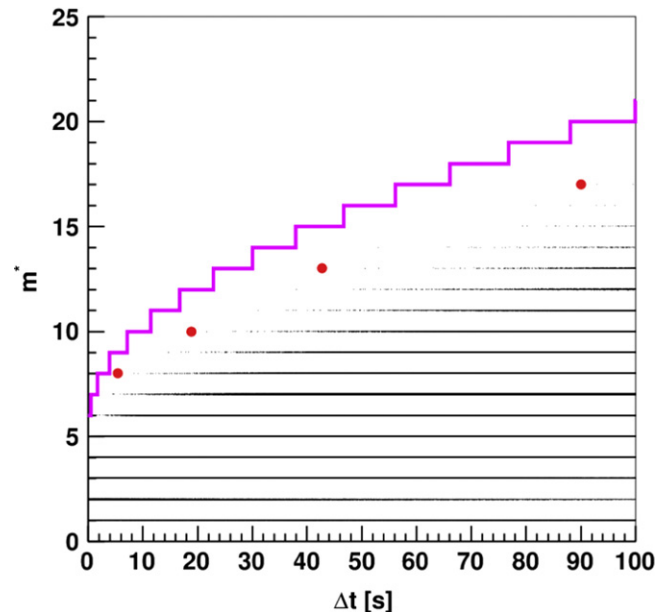
Bionta, R. M., Blewitt, G., Bratton, C. B., et al. (IMB collaboration) 1987, PhRvL, 58, 1494

Colgate, S. A., & White, R. H. 1966, ApJ, 143, 626

Domogatsky, G. V., & Zatsepin, G. T. 1965, in Proceedings of the IX International Cosmic Ray Conference, Vol. 1 (London: IUPAP), 1030

Falk, S. W. 1978, ApJL, 225, L133

Fukugita, M., Kohyama, Y., & Kubodera, K. 1988, PhLB, 212, 139

Fulgione, W., Mengotti-Silva, N., & Panaro, L. 1996, NIMPA, 368, 512

Gamow, G., & Schoenberg, M. 1940, PhRv, 58, 1117

Hirata, K., Kajita, T., Koshiba, M., et al. 1987, PhRvL, 58, 1490

Ikeda, M., Takeda, A., Fukuda, Y., et al. (The Super-Kamiokande collaboration) 2007, ApJ, 669, 519

Imshennik, V. S., & Ryazhskaya, O. 2004, AstL, 30, 14

Klein, R. I., & Chevalier, R. A. 1978, ApJL, 223, L109

Kolbe, E., & Langanke, K. 2001, PhRvC, 63, 025802

Loredo, T. J., & Lamb, D. Q. 2002, PhRvD, 65, 063002

LVD Collaboration 1993, in Proc. 23rd International Cosmic Ray Conference, Vol. 4 (Calgary: IUPAP), 468

LVD Collaboration 1995, in Proc. 24th International Cosmic Ray Conference, Vol. 1 (Rome: IUPAP), 762

LVD Collaboration 1997, in Proc. 25th International Cosmic Ray Conference, Vol. 7 (Durban: IUPAP), 33

LVD Collaboration 1999, in Proc. 26th International Cosmic Ray Conference, Vol. 2 (Salt Lake City: IUPAP), 223

LVD Collaboration 2001, in Proc. 27th International Cosmic Ray Conference, Vol. 230 (Hamburg: IUPAP), 1093

LVD Collaboration 2003, in Proc. 28th International Cosmic Ray Conference (Tsukuba: IUPAP), 1333

LVD Collaboration 2005, in Proc. 29th International Cosmic Ray Conference, Vol. 5 (Pune: IUPAP), 59

LVD Collaboration 2007, in Proc. 30th International Cosmic Ray Conference, Vol. 5 (Merida: IUPAP), 1425

LVD Collaboration 2009, in Proc. 31st ICRC (Lodz)

LVD Collaboration 2011, in Proc. 32nd International Cosmic Ray Conference, Vol. 4 (Beijing: IUPAP), 181

LVD Collaboration 2013, in Proc. 33rd International Cosmic Ray Conference (Rio de Janeiro: IUPAP) in press

Mikheev, S. P., & Smirnov, A. Y. 1985, SvJNP, 42, 913

Nadyozhin, D. K. 1977, Ap&SS, 49, 399

Nadyozhin, D. K. 1978, Ap&SS, 53, 131

Nakazato, K., Sumiyoshi, K., Suzuki, H., & Yamada, S. 2008, PhRvD, 78, 083014

Novoseltseva, R. V., Boliev, M. M., Volchenko, V. I., et al. 2011, Proceedings of the XXXII International Cosmic Ray Conference, Vol 4 (Beijing: IUPAP), 153

O'Connor, E., & Ott, C. D. 2011, ApJ, 730, 70

Pagliaroli, G., Vissani, F., Coccia, E., & Fulgione, W. 2009a, PhRvL, 103, 031102

Pagliaroli, G., Vissani, F., Costantini, M. L., & Ianni, A. 2009b, APh, 31, 163

Strumia, A., & Vissani, F. 2003, PhLB, 564, 42

Strumia, A., & Vissani, F. 2010, arXiv:hep-ph/0606054

Toivanen, J., Kolbe, E., Langanke, K., Martinez-Pinedo, G., & Vogel, P. 2001, NuPhA, 694, 395

Wolfenstein, L. 1978, PhRvD, 17, 2369

Woosley, S., & Janka, T. 2005, NatPh, 1, 147

Zel'dovich, Ya. B., & Guseinov, O. K. 1965, SPhD, 10, 524

Zichichi, A. 2000, Subnuclear Physics in World Scientific Series in 20th Century Physics, Vol. 24, The First 50 Years : Highlights from Erice to ELN, ed. O. Barnabei, P. Pupillo, & F. Roversi Monaco (Singapore: World Scientific)